

EXACT UPSCALING OF TRANSPORT IN POROUS MEDIA AND ITS APPLICATIONS

YALCHIN EFENDIEV *

Abstract. In this work I consider the exact upscaling of the transport in layered porous media. Some applications of the upscaled equation is discussed.

1. Introduction

The upscaling of the transport phenomena plays an important role in many applications, flow in porous media, turbulent diffusion just to name a few. For the flow in heterogeneous reservoirs it is usually the case that the level of detail incorporated into geologic characterization of reservoirs typically exceeds the capabilities of traditional flow simulators by a wide margin. For this reason, the upscaled models play an important role in the simulation. Developing an upscaled equation for the transport of mass in porous media has been under extensive study (see e.g. [1, 2, 3, 5, 11, 15, 16, 7, 17, 18, 20, 4, 21, 9, 8, 10, 12, 13, 14]). Some of the approaches use stochastic framework in deriving the average equations. A number of assumptions in the derivation of the average equations in the stochastic framework are usually made. Among them stationarity of the velocity field and the scale separation are common. These kinds of assumptions do not hold in general. For example, strong heterogeneities of the reservoir can cause the large variations in the velocity field. Moreover, due to the effects of the boundaries of the global domain the assumption about the stationarity can also be violated in the neighborhood of the boundaries. In the derivation of the upscaled equations in stochastic framework one usually neglects the effects of higher order terms in order to have closed system. The effects of these terms can be significant in general cases.

In this work I derive the the exact upscaled equation for the transport equation in layered porous media. The main idea in deriving of the upscaled equation is to find the form of this upscaled equation. The upscaled equation in this case contains the unknown parameters. To find these unknown parameters we use the average profile of the solution. Obtained in this way the upscaled equation is the exact upscaled equation for the transport in layered media. In this work I also compare our results with the results where the effects of the higher order correlations are neglected. For the layered system with two distinct velocities this comparison show that the difference between the upscaled models is in the velocity which counts for the memory effects.

The upscaled equation obtained in this work contains macro-diffusion (see Tartar, [19]). The macro-diffusion (often also called "macro-dispersion") has been investigated in literature under the different assumptions. Many attempts have been made to understand the dispersive behavior of the transport phenomena in literature. There are large number of works in many fields studying this dispersive behavior. Further in the work the simplification of exact upscaled equation for different special cases is considered. In particular for the application we obtain the approximation of the upscaled equation for the velocity fields whose variances are small.

As for the application of the upscaled model obtained in this work we consider the single phase flow in general porous media. In the upscaling of this problem it is often important to develop

*Institute for Mathematics, 400 Lind Hall, Univeristy of Minnesota, Minneapolis, MN 55455

the upscaling model on the coarse grid. Upscaling procedure are commonly used to coarsen the highly detailed structure of the velocity field to the scales suitable for the flow simulation. This is performed by dividing the domain into the coarse blocks where the velocity can be approximated by its average value. Our approach in this case is needed to be applied to each coarse block. The nonuniform coarsening approach plays an important role in applying our approach to the flow in general porous media. The idea of nonuniform coarsening method is to capture high extremes of the velocity through the use of a nonuniform coarsening methodology. This procedure introduces grid refinement in regions likely to lead to high velocities while maintaining a coarser grid structure in less active regions. The advantage of nonuniform coarsening is that this approach tends to minimize the variation of the velocity field in each coarse block. This allows us to use the average equations for the small variances in each coarse block.

The paper is organized as follows. In the next section we describe the governing equation and derive the exact averaged equation. The section 3 is devoted to the approximation of the averaged equations for the velocity fields with small variances. In the last section an approximate upscaling method obtained in the previous sections is applied for the general flow scenarios.

2. Governing equations and the exact averaged equation

The equations governing single phase displacements on the fine scale are the usual Darcy's law coupled with mass conservation. These equations in terms of the dimensionless pressure and saturation as follows:

$$\nabla \cdot \mathbf{v} = 0, \quad \mathbf{v} = -\mathbf{k}\nabla p \quad (2.1)$$

$$\frac{\partial S}{\partial t} + \mathbf{v} \cdot \nabla S = 0, \quad (2.2)$$

where \mathbf{k} is the permeability describing the heterogeneity of the porous media, \mathbf{v} is the velocity field and S is the saturation. The average equation for the pressure field is of the same form as the fine scale pressure equation with an averaged permeability tensor, \mathbf{k}^* , replaces the fine grid \mathbf{k} in (2.1). It has been known in literature that the upscaled equation for the saturation contains diffusive terms. This terms depends on the statistical properties of the velocity field. In many cases the diffusive terms have been approximated under different assumptions. Here we would like to present the upscaled equation for the saturation in the layered media without any prior assumptions. For further analysis the velocity field is denoted by $\mathbf{v} = (v_x, v_y)$, where $v_x = v(y)$, and $v_y = 0$.

Before discussing the upscaled model we would like to present the averaged equation derived when the velocity field is almost uniform [4, 21]. The common technique deriving the averaged equation in this case is the use of the expansion of the velocity field around its mean value, $\mathbf{v} = \bar{\mathbf{v}} + \mathbf{v}'$. Assuming v' is small, after some manipulations the following upscaled equation can be derived

$$\frac{\partial \bar{S}}{\partial t} + \bar{v}_j \nabla_j \bar{S} = \nabla_k \int_0^t \overline{v'_k(\mathbf{x})v'_j(\mathbf{x} - \bar{\mathbf{v}}(t - \tau))} \nabla_j \bar{S}(\tau, \mathbf{x} - \bar{\mathbf{v}}(t - \tau)) d\tau, \quad (2.3)$$

where $\overline{v'_k(\mathbf{x})v'_j(\mathbf{y})}$ is the correlation of the velocity at points \mathbf{x} and \mathbf{y} . For the layered case this equation can be simplified taking into account that

$$\overline{v'_k(\mathbf{x})v'_j(\mathbf{x} - \bar{\mathbf{v}}(t - \tau))} = var(v).$$

The upscaled equation for this case is

$$\frac{\partial \bar{S}}{\partial t} + \bar{v} \frac{\partial \bar{S}}{\partial x} = \text{var}(v) \int_0^t \frac{\partial^2 \bar{S}}{\partial x^2}(\tau, x - \bar{v}(t - \tau)) d\tau. \quad (2.4)$$

To derive the exact upscaled model we assume that there are n layers (in x direction) with the velocities v_i ($i = 1, \dots, n$), and with the fraction m_i ($i = 1, \dots, n$). The average profile of the saturation at each point x is then defined as the arithmetical average of the saturation along y direction,

$$\bar{S} = \int_0^{L_y} S(x, y, t) dy. \quad (2.5)$$

For the discrete case \bar{S} can be written as

$$\bar{S} = \sum_{i=1}^n m_i H(x - v_i t), \quad (2.6)$$

where $H(x - v_i t)$ is the solution of a single wave equation :

$$\frac{\partial H}{\partial t} + v_i \frac{\partial H}{\partial x} = 0.$$

For our calculations the nature of the function H is not important.

First we derive the upscaled equation for the two layered case with velocities v_1, v_2 and volume fractions m_1, m_2 . In this case the average saturation profile is

$$\bar{S} = m_1 H(x - v_1 t) + m_2 H(x - v_2 t). \quad (2.7)$$

The idea of the deriving the upscaled equations here is to look for them apriori knowing their form. Then our goal is to find the unknown parameters in the upscaled equation. This turns out to be easy for the case of two layers, but more complicated in general. In the case of two layers we look for the averaged equation in the form (2.4) with unknowns \bar{v} , D and u . In particular, we assume that \bar{S} satisfies

$$\frac{\partial \bar{S}}{\partial t} + \bar{v} \frac{\partial \bar{S}}{\partial x} = D \int_0^t \frac{\partial^2 \bar{S}}{\partial x^2}(\tau, x - u(t - \tau)) d\tau. \quad (2.8)$$

Substituting (2.7) into (2.8) we have

$$\begin{aligned} m_1(\bar{v} - v_1)H'(x - v_1 t) + m_2(\bar{v} - v_2)H'(x - v_2 t) = \\ D \int_0^t \left(m_1 H''(x - u(t - \tau) - v_1 \tau) + m_2 H''(x - u(t - \tau) - v_2 \tau) \right) d\tau. \end{aligned} \quad (2.9)$$

Further the r.h.s of (2.9) can be simplified in the following manner

$$\begin{aligned} D \int_0^t \left(\frac{m_1}{u - v_1} \frac{d}{d\tau} H'(x - u(t - \tau) - v_1 \tau) + \frac{m_2}{u - v_2} \frac{d}{d\tau} H'(x - u(t - \tau) - v_2 \tau) \right) d\tau = \\ D \left(\frac{m_1}{u - v_1} H'(x - v_1 \tau) + \frac{m_2}{u - v_2} H'(x - v_2 \tau) - \left(\frac{m_1}{u - v_1} + \frac{m_2}{u - v_2} \right) H'(x - u(t - \tau)) \right). \end{aligned} \quad (2.10)$$

The equality between the l.h.s of (2.9) and the r.h.s. of (2.10) gives us the following three relations:

$$\begin{aligned} \frac{m_1}{u - v_1} + \frac{m_2}{u - v_2} &= 0; \\ D \frac{m_1}{u - v_1} &= m_1(\bar{v} - v_1); \quad D \frac{m_2}{u - v_2} = m_2(\bar{v} - v_2); \end{aligned}$$

The first equation defines the memory speed u , $u = m_1 v_2 + m_2 v_1$. From the last two equations we easily derive that $\bar{v} = m_1 v_1 + m_2 v_2$ and $D = \text{var}(v)$. Thus the the exact upscaled equation in this case is

$$\frac{\partial \bar{S}}{\partial t} + \bar{v} \frac{\partial \bar{S}}{\partial x} = \text{var}(v) \int_0^t \frac{\partial^2 \bar{S}}{\partial x^2}(\tau, x - (m_1 v_2 + m_2 v_1)(t - \tau)) d\tau. \quad (2.11)$$

Comparing (2.4) and (2.11) we see that the approximate upscaled equation differs from the exact one only in the memory speed. In (2.4), the memory speed is $m_1 v_1 + m_2 v_2$, while in (2.11) the memory speed is $m_1 v_2 + m_2 v_1$.

For the general case when the porous media contains n layers we look for the upscaled equation in the following form

$$\frac{\partial \bar{S}}{\partial t} + \bar{v} \frac{\partial \bar{S}}{\partial x} = \sum_{i=1}^{n-1} \int_0^t \beta_i \frac{\partial^2}{\partial x^2} \bar{S}(x - u_i(t - \tau), \tau) d\tau \quad (2.12)$$

where \bar{v} , β_i , and u_i ($i = 1, \dots, n - 1$) are unknowns. This is somehow analogous to the case of two layers. Substituting the expression for the averaged saturation profile (2.6) into (2.12) we have

$$\sum_{k=1}^n m_k (\bar{v} - v_k) H'(x - v_k t) = \sum_{k=1}^n \sum_{i=1}^{n-1} m_k \beta_i \int_0^t \frac{\partial^2}{\partial x^2} H(x - u_i(t - \tau) - v_k \tau) d\tau. \quad (2.13)$$

Similar to the case of two velocities we can simplify the r.h.s. of (2.13) in the following way

$$\begin{aligned} \sum_{k=1}^n \sum_{i=1}^{n-1} m_k \beta_i \int_0^t \frac{1}{u_i - v_k} \frac{d}{d\tau} H'(x - u_i(t - \tau) - v_k \tau) d\tau = \\ \sum_{k=1}^n \left(\sum_{i=1}^{n-1} m_k \beta_i \frac{1}{u_i - v_k} \right) H'(x - v_k \tau) - \sum_{i=1}^{n-1} \left(\sum_{k=1}^n m_k \beta_i \frac{1}{u_i - v_k} \right) H'(x - u_i \tau). \end{aligned} \quad (2.14)$$

Further, equating the l.h.s. of (2.13) and the r.h.s. of (2.14) we have the following relations for our unknown parameters \bar{v} , β_i , and u_i ($i = 1, \dots, n - 1$)

$$\begin{aligned} \sum_{k=1}^n m_k \beta_i \frac{1}{u_i - v_k} &= 0, \quad i = 1, \dots, n - 1 \\ \sum_{i=1}^{n-1} m_k \beta_i \frac{1}{u_i - v_k} &= m_k (\bar{v} - v_k), \quad k = 1, \dots, n. \end{aligned}$$

Note that there are $2n - 1$ equations for $2n - 1$ unknowns \bar{v} , β_i , and u_i ($i = 1, \dots, n - 1$). The above expressions are equivalent to

$$\sum_{k=1}^n \frac{m_k}{u_i - v_k} = 0, \quad (2.15)$$

$$\sum_{i=1}^{n-1} \frac{\beta_i}{u_i - v_k} = (\bar{v} - v_k). \quad (2.16)$$

As it can be seen the $n - 1$ equations in(2.15) define the values of u_i ($i = 1, \dots, n - 1$). The n equations in (2.16) define the values of β_i , ($i = 1, \dots, n - 1$), and \bar{v} . The value of \bar{v} can be readily calculated by multiplying (2.16) to m_k and summing over k ,

$$\sum_{k=1}^n m_k (\bar{v} - v_k) = \sum_{k=1}^n \sum_{i=1}^{n-1} m_k \frac{\beta_i}{u_i - v_k}.$$

The r.h.s of this equality is zero because of (2.15). Thus,

$$\bar{v} = \sum_{k=1}^n m_k v_k,$$

i.e., the mean value of the velocity. From (2.15) one can find that u_i ($i = 1, \dots, n - 1$) satisfy

$$\sum_{k=1}^n m_k \prod_{p \neq k, p=1}^{n-1} (u_i - v_p) = 0.$$

This indicates that u_i ($i = 1, \dots, n - 1$) are the roots of the following polynomial of the degree $n - 1$

$$R(z) = \sum_{k=1}^n m_k \prod_{p \neq k, p=1}^{n-1} (z - v_p) = 0.$$

Next we show that the roots of the polynomial $R(z)$ are between the values of v_i , i.e.,

$$v_1 \leq u_1 \leq v_2 \leq u_2 \leq \dots \leq u_{n-1} \leq v_n.$$

Indeed, it is easy to show that $R(z)$ is changes sign from v_i to v_{i+1} , i.e., $R(v_i)R(v_{i+1}) \leq 0$. Consequently, the roots of the polynomial $R(z)$ are between the values of v_i .

It is more difficult to understand β_i ($i = 1, \dots, n - 1$) based on the equations (2.16). In particular, we are interested to derive the expressions for the averaged properties of β_i and their high moments. For this reason we present the following identity for all z :

$$\left(\sum_{k=1}^n \frac{m_k}{z - v_k} \right)^{-1} - z + \bar{v} = \sum_{i=1}^{n-1} \frac{\beta_i}{u_i - z}. \quad (2.17)$$

To show the (2.17) holds we note that (2.17) can be written as a polynomial of the degree less than $2n - 1$. This polynomial has degree $2n - 1$ when all v_i 's ($i = 1, \dots, n$) are different. To show that the identity (2.17) holds for the case of different v_i 's we note that the identity holds for $z = v_i$, ($i = 1, \dots, n$), and for $z = u_i$, ($i = 1, \dots, n - 1$). Indeed, it can be verified that for the values of $z = v_i$ ($i = 1, \dots, n$) the identity (2.17) becomes the identity (2.16) and for the values of $z = u_i$ ($i = 1, \dots, n - 1$) the identity (2.17) becomes the identity (2.15). These are $2n - 1$ different values for z when the identity holds. Thus it holds for all z . Let's note that in the case when some of the values of v_i are coincide then the degree of the polynomial decreases accordingly. It can be checked

in the above way that the identity (2.17) holds for the values of $z = u_i$, ($i = 1, \dots, n-1$) and for the values of $z = v_i$, ($i = 1, \dots, n$). This is sufficient for the fact that the identity holds for all z .

To calculate the moments of β_i 's we write the l.h.s. of (2.17) as

$$\frac{B_n z^n + B_{n-1} z^{n-1} + B_{n-2} z^{n-2} + B_{n-3} z^{n-3} + P_{n-4}(z)}{\sum_{k=1}^n m_k \prod_{i=1, i \neq k}^n (z - v_i)} \quad (2.18)$$

where $P_{n-4}(z)$ is a polynomial of the degree $n-4$. The coefficients B_i ($i = n-3, \dots, n$) can be calculated:

$$B_n = 0, \quad B_{n-1} = 0;$$

after some algebra:

$$B_{n-2} = \text{var}(v);$$

$$B_{n-3} = -\sum_{i=1}^n m_i v_i^2 \sum_{i=1}^n v_i + \sum_{i=1}^n m_i v_i^3 + \left(\sum_{i=1}^n m_i v_i \right)^2 \sum_{i=1}^n v_i - \sum_{i=1}^n m_i v_i \sum_{i=1}^n m_i v_i^2.$$

On the other hand the r.h.s. of (2.17) is

$$\frac{\sum_{k=1}^{n-1} \beta_k \prod_{i=1, i \neq k}^n (z - u_i)}{\prod_{i=1}^{n-1} (z - u_i)}. \quad (2.19)$$

It can be shown that

$$\prod_{i=1}^{n-1} (z - u_i) = \sum_{k=1}^n m_k \prod_{i=1, i \neq k}^n (z - v_i) \quad (2.20)$$

since they coincide at $z = u_i$ ($i = 1, \dots, n-1$). The equality of (2.18) and (2.19) along with (2.20) gives

$$B_n z^n + B_{n-1} z^{n-1} + B_{n-2} z^{n-2} + B_{n-3} z^{n-3} + P_{n-4}(z) = \sum_{k=1}^{n-1} \beta_k \prod_{i=1, i \neq k-1}^n (z - u_i). \quad (2.21)$$

From where it can be easily derived that

$$\sum_{i=1}^{n-1} \beta_i = B_{n-2} = \text{var}(v), \quad (2.22)$$

and after some algebra

$$\sum_{i=1}^{n-1} \beta_i (u_i - \bar{v}) = \sum_{i=1}^n m_i v_i^3 - \bar{v} \sum_{i=1}^n m_i v_i^2 - 2\text{var}(v)\bar{v}. \quad (2.23)$$

Note that the r.h.s. of the last equality is equal to the third moment of v_i 's which we denote $\text{skew}(v)$,

$$\text{skew}(v) = \sum_{i=1}^n m_i (v_i - \bar{v})^3.$$

Summarizing the above calculations we have derived the following upscaled equation for the n layered system:

$$\frac{\partial \bar{S}}{\partial t} + \bar{v} \frac{\partial \bar{S}}{\partial x} = \sum_{i=1}^{n-1} \int_0^t \beta_i \frac{\partial^2}{\partial x^2} \bar{S}(x - u_i(t - \tau), \tau) d\tau \quad (2.24)$$

where u_i are defined from (2.15) and β_i are defined from (2.16). We also found that the total diffusion ($\sum \beta_i$) is equal to $var(v)$.

This result can be generalized to the layered flow in any direction. The calculations are similar and we omit them here presenting the final result: Assuming that the direction of the layers are defined with angle θ we have:

$$\begin{aligned} \frac{\partial \bar{S}}{\partial t} + \cos(\theta) \bar{v} \frac{\partial \bar{S}}{\partial x} + \sin(\theta) \bar{v} \frac{\partial \bar{S}}{\partial y} = \\ \sum_{i=1}^{n-1} \int_0^t \beta_i \left(\cos(\theta) \frac{\partial}{\partial x} + \sin(\theta) \frac{\partial}{\partial y} \right)^2 \bar{S}(x - u_i(t - \tau) \cos(\theta), y - u_i(t - \tau) \sin(\theta) \tau) d\tau \end{aligned} \quad (2.25)$$

where u_i and β_i are defined as above.

Remark 2.1.

We would like to note that the parameters β_i , u_i , and \bar{v} in the averaged equation (2.24) (or (2.25) in general) depend on the overall statistical properties of the layered system.

Remark 2.2.

In applications one is often interested in the average flow rate at the production boundaries (the part of the total boundaries where $\mathbf{v} \cdot \mathbf{n} > 0$). The average flow rate at each time on this portion of the boundary is defined as

$$F(t) = \frac{\int_{S^{out}} \mathbf{v} \cdot \mathbf{n} S dl}{\int_{S^{out}} \mathbf{v} \cdot \mathbf{n} dl}$$

where S^{out} is the part of the total boundary where $\mathbf{v} \cdot \mathbf{n} > 0$. Assuming that all trajectories which start at the injection boundaries (the portion of the boundaries where $\mathbf{v} \cdot \mathbf{n} < 0$) and end at the production boundaries compose n layers with the velocities \mathbf{w}_i . Then we can approximate the average flux in the following form

$$F(t) = \sum_{i=1}^n q_i H(\mathbf{x} - \mathbf{w}_i t). \quad (2.26)$$

Here \mathbf{w}_i is an average velocity assigned to the trajectory i , and q_i is the flux carried with the trajectory i , ($i = 1, \dots, n$). Moreover, by the choice of w_i we can always achieve that the velocities \mathbf{w}_i are parallel, i.e., $\mathbf{w}_i = (w_i \cos(\theta), w_i \sin(\theta))$, for some θ for all i . Then the average flux $F(t)$ is defined by (2.25):

Remark 2.3. The upscaled equation derived in this work can be simplified for the layered system which has a small fraction of the layers with very high velocities. In this case the variance of the velocity field is large. It can be verified that in this case the sum of β_i corresponding to high values of the memory speeds u_i is almost $var(v)$. The upscaled equation in this case approximately is:

$$\frac{\partial \bar{S}}{\partial t} + \bar{v} \frac{\partial \bar{S}}{\partial x} = var(v) \int_0^t \frac{\partial^2}{\partial x^2} \bar{S}(x - u(t - \tau), \tau) d\tau, \quad (2.27)$$

where u can be taken to be the largest memory velocity.

3. Approximation of the upscaled equation for velocity fields with small variances

The approximation of the equation (2.24) for velocity fields with small variances plays an important role in application. In the next section using this approximation we propose a coarse model. To study the behavior of (2.24) for velocity fields with small $var(v)$ we write the r.h.s. of the upscaled equation using the integration by parts as

$$\begin{aligned} & \sum_{i=1}^{n-1} \beta_i \int_0^t \frac{d\tau}{d\tau} \frac{\partial^2}{\partial x^2} \bar{S}(x - u_i(t - \tau), \tau) d\tau = \\ & \sum_{i=1}^{n-1} \beta_i \tau \frac{\partial^2}{\partial x^2} \bar{S}(x - u_i(t - \tau), \tau) \Big|_{\tau=0}^{\tau=t} - \sum_{i=1}^{n-1} \beta_i \int_0^t \tau \frac{\partial^2}{\partial x^2} \frac{d}{d\tau} \bar{S}(x - u_i(t - \tau), \tau) d\tau. \end{aligned} \quad (3.1)$$

Further for the last term on the r.h.s. of (3.1) we have

$$\begin{aligned} \frac{d}{d\tau} \bar{S}(x - u_i(t - \tau), \tau) &= S_t(x - u_i(t - \tau), \tau) + u_i S_x(x - u_i(t - \tau), \tau) = \\ S_t(x - u_i(t - \tau), \tau) &+ \bar{v} S_x(x - u_i(t - \tau), \tau) + (u_i - \bar{v}) S_x(x - u_i(t - \tau), \tau) = \\ (u_i - \bar{v}) S_x(x - u_i(t - \tau), \tau) &+ O(var(v)). \end{aligned} \quad (3.2)$$

Thus (3.1) becomes:

$$\left(\sum_{i=1}^{n-1} \beta_i \right) t \frac{\partial^2}{\partial x^2} S(x, t) - \int_0^t \tau \sum_{i=1}^{n-1} \beta_i (u_i - \bar{v}) \frac{\partial^3}{\partial x^3} S(x - u_i(t - \tau), \tau) d\tau + O((var(v))^2). \quad (3.3)$$

According to (2.22) the sum of β_i 's is $var(v)$. The second term in (3.3) can be further approximated similar to (3.1) using the integration by parts. The result is

$$\left(\sum_{i=1}^{n-1} \beta_i \right) t \frac{\partial^2}{\partial x^2} S(x, t) - \frac{t^2}{2} \sum_{i=1}^{n-1} \beta_i (u_i - \bar{v}) \frac{\partial^3}{\partial x^3} S(x, t) + O((var(v))^2). \quad (3.4)$$

According to (2.23) the coefficient in front of the second term is $skew(v)$. Then the effective equation up to the third order is

$$\frac{\partial \bar{S}}{\partial t} + \bar{v} \frac{\partial \bar{S}}{\partial x} = var(v) t \frac{\partial^2}{\partial x^2} S(x, t) - skew(v) \frac{t^2}{2} \frac{\partial^3}{\partial x^3} S(x, t). \quad (3.5)$$

4. Numerical model for the upscaling of saturation

In this section we propose a numerical method for the upscaling of the saturation for general porous media. This method works in conjunction with nonuniform coarsening [9, 7, 8]. The idea of nonuniform coarsening method is to capture high extremes of the velocity through use of a nonuniform coarsening methodology. This procedure introduces grid refinement in regions likely to lead to high velocities (and early breakthrough) while maintaining a coarser grid structure in less active regions. The other advantage of nonuniform coarsening is that this approach tends to minimize the variation of the velocity field in each coarse block. This allows us to use the approximation derived in the previous section in each coarse block. The nonuniform coarsening alone approximates the

motion of the saturation in each coarse block by the averaged front neglecting the small variations in the velocity field. These variations are the cause of early breakthrough times. Introducing the additional higher order fluxes we take into account small variations of the velocity field to some extent.

In our numerical model we use

$$\frac{\partial \bar{S}}{\partial t} + \bar{v} \frac{\partial \bar{S}}{\partial x} = var(v)t \frac{\partial^2}{\partial x^2} S(x, t) \quad (4.1)$$

as an approximation of the saturation in each coarse block. We assume that in each coarse block the flow is strongly correlated along the average flow direction of the coarse block. This is usually case for the high degree of nonuniform coarsening. Otherwise one needs to calculate $var(v)$ according to Remark 2.2.

The difficulty in this modeling is to set initial time for the calculation of the diffusive flux in each coarse block. In general the flux entering into the each coarse block is nonuniform. In this case it is difficult to set a good starting time for the diffusive flux in each coarse block since the flux into the coarse block changes continuously. In the case of nonuniform coarsening on the other hand the large portion of the flux enters into a coarse block at a certain time. This approximately localize the time when the flux enters in to the coarse block. As a the starting time for the diffusive flux at each coarse block we define the time when the flux into the coarse block is almost equal to the total flux into this coarse block. The reason for choosing almost equality of the fluxes is numerical diffusion in our methods. We use second order method to discretize the convective part of the averaged equations.

In our computations we compare the total volumetric flow through the system. The saturation is given in a rectangle domain with the sides $L_x = 5.0$ and $L_z = 1.0$. The permeability fields we use in this paper are identical, except for the statistically generated absolute permeability field. The flow domain is a rectangle whose length is five times larger than its thickness. The fine grid in all cases is a uniform 100×100 rectangular grid. Commonly used variogram for the distribution of the permeability field is the exponential variogram. In our numerical experiments we use exponential variogram for the realizations of the permeability field. The exponential variogram is defined by the two correlation lengths, in vertical direction, l_z , and horizontal direction, l_x , and the variance of the permeability field, σ . To generate an individual realization of permeability field we use GSLIB (see [6]). This routine uses the sequential Gaussian simulation.

In our numerical experiments we choose the permeability fields with the variances from $\sigma = 0.5$ up to $\sigma = 1.0$. Depending on the value of the σ the degree of the coarsening can change. Our goal is to have in each block the variance to be small. The coarsening of order 15×15 is sufficient for our purposes. Here for simplicity we only present the case with long correlation lengths in the mean flow direction and the small correlation length in the cross direction. In particular the correlation lengths are chosen to be $l_x = 1.5$, $l_z = 0.01$.

The average equation with diffusion requires an additional boundary conditions at the injection and the production boundaries of the whole reservoir. We assume that only convective fluxes entering and leaving the domain of the whole reservoir, i.e., we apply the higher order fluxes strictly in the interior of the reservoir.

Our first example Fig. 5.1 is for the case $l_x = 0.15$, $l_z = 0.01$, $\sigma = 0.5$. In this and all subsequent figures, the 100×100 fine grid results are indicated by the dashed-dotted line, the coarse grid results using nonuniform coarsening only with no diffusive flux by the dotted line and the coarse grid results using our upscaling model for dispersivity by the solid line. In this case, the coarse models are of

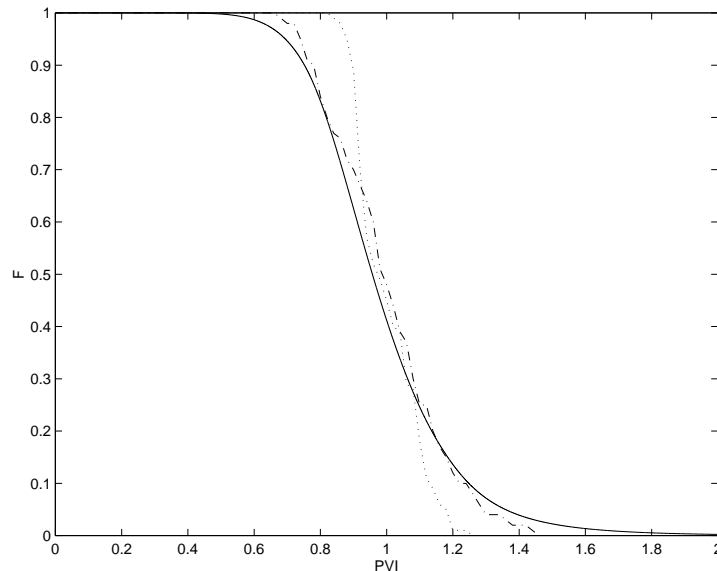


FIG. 5.1. Case $l_x = 0.15$, $l_z = 0.01$, $\sigma = 0.5$. Dashed-dotted line is for fine fractional flow curve on 100×100 grid, dotted line is for coarse model using non-uniform coarsening method on 12×10 coarse grid, solid line is for the coarse model with diffusion on the same coarse grid

dimension 12×10 (in the nonuniform coarsening procedure we do not specify the exact dimensions of the coarse model, so these dimensions are typically not “round” numbers). The improvement using our approximate coarse model is evident from this plot. In Fig. 5.2 we consider the same fine grid realization but introduce lower levels of upscaling in the coarse model (the coarse model in this case is 14×13). The same behaviors are evident in this Figure.

We next consider a case with a larger variance of the permeability field. In Fig.5.3 and Fig. 5.4 we plot the numerical results on the coarse grids 12×11 and 15×15 respectively. As we see from these figures that one gets an improved result using our upscaling model.

In our final examples (Fig. 5.5 and Fig. 5.6 the variance of the permeability field is further increased. The improvement in these figures are evident.

5. Conclusions

One of the goals in deriving the exact upscaled equation in the above manner was to apply the above procedure to the nonlinear problems, i.e., the hyperbolic equations with nonlinear fluxes (e.g., Buckley-Leverett equations). Unfortunately, I have not succeeded in that.

REFERENCES

- [1] J. Barker and S. Thibeau. A critical review of the use of pseudo-relative permeabilities for upscaling. *SPE Res. Eng.*, pages 138–143, 1997.
- [2] R. Beckie, A.A. Aldama, and E.F. Wood. Modeling the large-scale dynamics of saturated groundwater flow using spatial filtering theory: 1. theoretical development. *Water Resour. Res.*, 32:1269–1280, 1996.
- [3] M. A. Christie. Upscaling for reservoir simulation. *J. Pet. Tech.*, 48:1004–1010, 1996.
- [4] G. Dagan. Solute transport in heterogeneous porous formations. *J. Fluid Mech.*, 145:151, 1984.

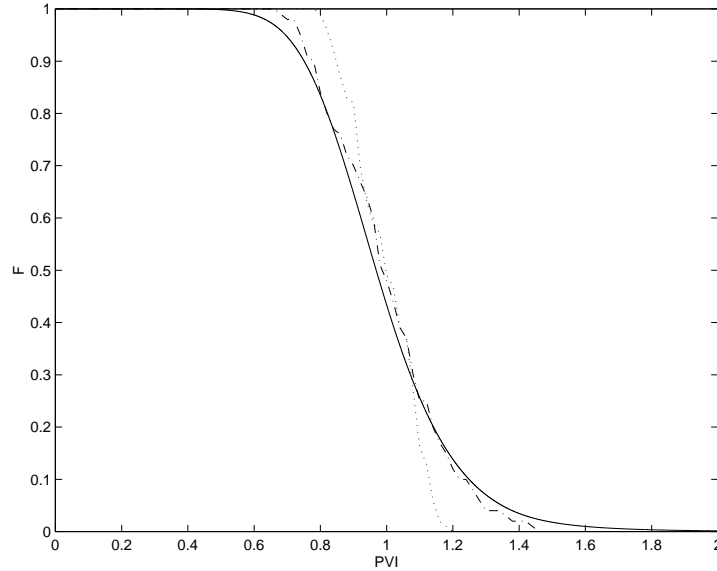


FIG. 5.2. Case $l_x = 0.15$, $l_z = 0.01$, $\sigma = 0.5$. Dashed-dotted line is for fine fractional flow curve on 100×100 grid, dotted line is for coarse model using non-uniform coarsening method on 14×13 coarse grid, solid line is for the coarse model with diffusion on the same coarse grid

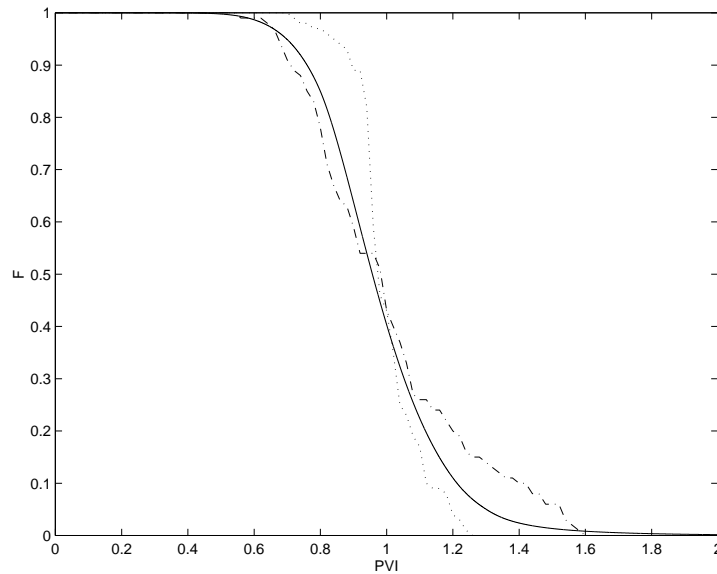


FIG. 5.3. Case $l_x = 0.15$, $l_z = 0.01$, $\sigma = 0.75$. Dashed-dotted line is for fine fractional flow curve on 100×100 grid, dotted line is for coarse model using non-uniform coarsening method on 12×11 coarse grid, solid line is for the coarse model with diffusion on the same coarse grid

- [5] G. Dagan. Theory of solute transport by groundwater. *Ann. Rev. Fluid Mech.*, 19:183–215, 1987.
- [6] C. V. Deutsch and A.G. Journel. *GSLIB - Geostatistical software library - User's guide - Version 1*. Stanford Univeristy, 1991.
- [7] L. J. Durlofsky. Use of higher moments for the description of upscaled, process independent relative permeabilities. *SPE*, pages 474–484, 1997a.

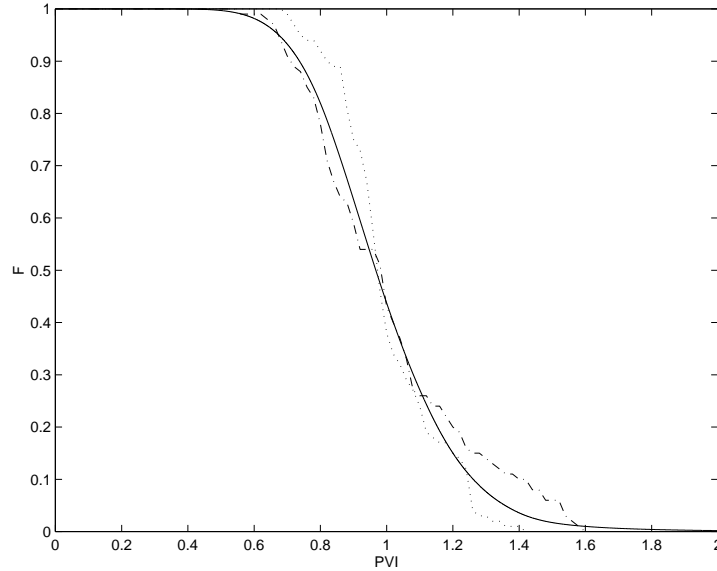


FIG. 5.4. Case $l_x = 0.15$, $l_z = 0.01$, $\sigma = 0.75$. Dashed-dotted line is for fine fractional flow curve on 100×100 grid, dotted line is for coarse model using non-uniform coarsening method on 15×15 coarse grid, solid line is for the coarse model with diffusion on the same coarse grid

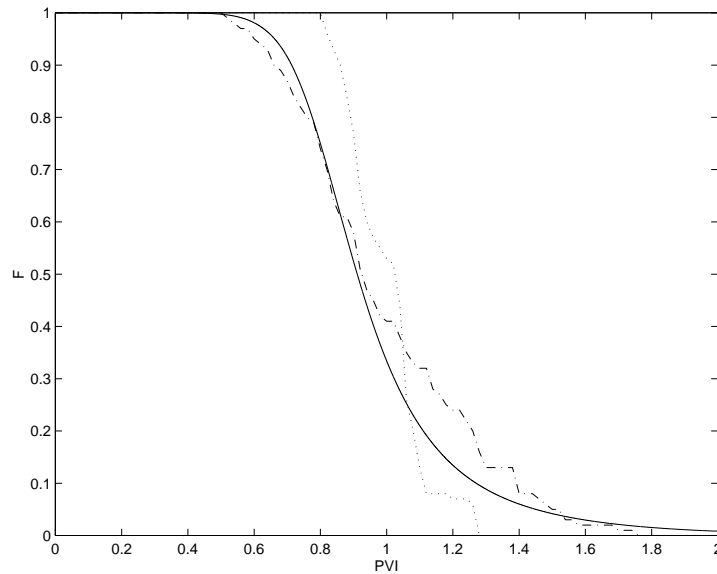


FIG. 5.5. Case $l_x = 0.15$, $l_z = 0.01$, $\sigma = 0.8$. Dashed-dotted line is for fine fractional flow curve on 100×100 grid, dotted line is for coarse model using non-uniform coarsening method on 14×12 coarse grid, solid line is for the coarse model with diffusion on the same coarse grid

- [8] L. J. Durlofsky. Coarse scale models of two phase flow in heterogeneous reservoirs: Volume averaged equations and their relationship to the existing upscaling techniques. *Computational Geosciences*, 1999. to appear.
- [9] L. J. Durlofsky, R. A. Behrens, R. C. Jones, and A. Bernath. Scale up of heterogeneous three dimensional reservoir descriptions. *SPE Journal*, pages 313–326, 1996.
- [10] Y. R. Efendiev. The multiscale finite element method and its applications. Ph.D. thesis, California Institute of

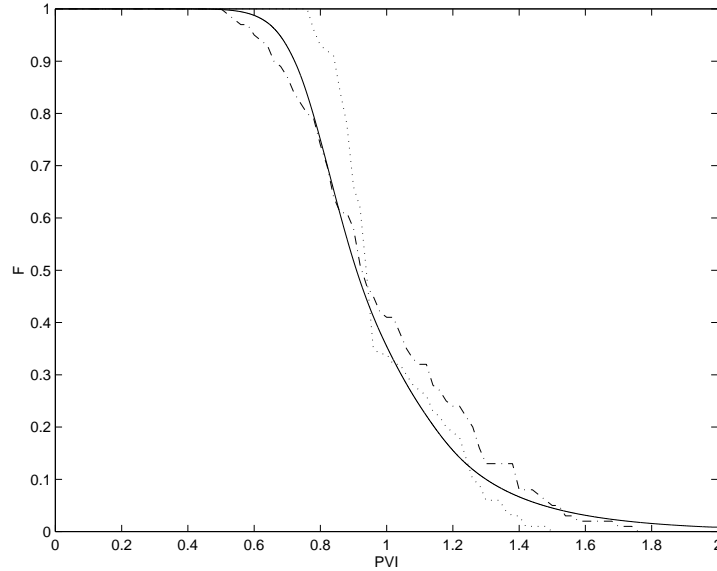


FIG. 5.6. Case $l_x = 0.15$, $l_z = 0.01$, $\sigma = 0.8$. Dashed-dotted line is for fine fractional flow curve on 100×100 grid, dotted line is for coarse model using non-uniform coarsening method on 16×15 coarse grid, solid line is for the coarse model with diffusion on the same coarse grid

Technology, 1999.

- [11] W. Graham and D. McLaughlin. Stochastic analysis of nonstationary subsurface solute transport. 1. unconditional moments. *Water Resour. Res.*, 25:215–232, 1989.
- [12] T. Y. Hou and X. H. Wu. A multiscale finite element method for elliptic problems in composite materials and porous media. *Journal of Computational Physics*, 134:169–189, 1997.
- [13] P. Indelman. On coarse grids simulation of solute transport in heterogeneous formations. In T. H. Dracos and F. Stauffer, editors, *Transport and Reactive Processes in Aquifers*, pages 317–322. Balkema, Rotterdam, 1994.
- [14] P. Indelman. On coarse grids simulation of solute transport in heterogeneous formations. In T. H. Dracos and F. Stauffer, editors, *Transport and Reactive Processes in Aquifers*, pages 317–322. Balkema, Rotterdam, 1994.
- [15] P. Kitanidis. Prediction by the method of moments of transport in a heterogeneous formation. *J. Hydrology*, 102:453–473, 1988.
- [16] S. Neuman. Eulerian-lagrangian theory of transport in space-time nonstationary velocity fields: Exact nonlocal formalism by conditional moments and weak approximation. *Water Resour. Res.*, 29:633–645, 1993.
- [17] Y. Rubin. Stochastic modeling of macrodispersion in heterogeneous porous media. *Water Resour. Res.*, 26:133–141, 1990.
- [18] Y. Rubin, A. Sun, R. Maxwell, and A. Bellin. The concept of block-effective macrodispersivity and a unified approach for grid-scale- and plume-scale-dependent transport. *J. Fluid Mech.*, 395:161–180, 1999.
- [19] L. Tartar. Nonlocal effects induced by homogenization. *PDE and calculus of variations*, pages 925–938, 1989. Boston.
- [20] D. Zhang, L. Li, and H.A. Tchelepi. Stochastic formulation for uncertainty assessment of two-phase flow in heterogeneous reservoirs. *SPE 51930*, 1999.
- [21] Qiang Zhang. The asymptotic scaling behavior of mixing induced by a random velocity field. *Advances in Applied Math*, 16:23–58, 1995.